Repulsion Effect on Superinfecting Virions by Infected Cells

Xiulan Lai · Xingfu Zou

Abstract In this paper, the repulsion effect of superinfecting virion by infected cells is studied by a reaction diffusion equation model for virus infection dynamics. In this model, the diffusion of virus depends not only on its concentration gradient but also on the concentration of infected cells. The basic reproduction number, linear stability of steady states, spreading speed and existence of traveling wave solutions for the model are discussed. It is shown that viruses spread more rapidly with the repulsion effect of infected cells on superinfecting virions, than with random diffusion only. For our model, the spreading speed of free virus is not consistent with the minimal traveling wave speed. With our general model, numerical computations of the spreading speed show that the repulsion of superinfecting virion promotes the spread of virus, which confirms, not only qualitatively but also quantitatively, the experimental result of Doceul et al. (Science 327:873–876, 2010).

1 Introduction

Viruses are usually thought to spread across susceptible cells through an iterative process, consisting of attachment to a target cell, entry, replication and release of new virions, which then move on to infect other uninfected target cells. According to

X. Lai · X. Zou (✉)
Department of Applied Mathematics, University of Western Ontario, London, ON N6A 5B7, Canada
e-mail: xzou@uwo.ca

such an understanding, the spreading speed of virus would be limited by how quickly virus can reproduce in infected cells. However, a recent study published in *Science* (Doceul et al. 2010) reveals that vaccinia virus spreads much faster than previously thought. Using live video microscopy, Doceul et al. (2010) found that the vaccinia virus was spreading across one cell fourfold faster than its replication cycle should allow. Indeed, vaccinia virus spreads across one cell every 1.2 h on average, but in vaccinia viral replication kinetics, new virions are formed only 5–6 h after infection, or in virus-induced cell motility, a cell starts to move 5–6 h after infection.

In seeking an explanation for this phenomenon, a new mechanism was discovered, that is, the repulsion of superinfecting virions by infected cells (Doceul et al. 2010). Indeed, a peculiar feature of vaccinia infection is the formation of actin tails, which propel virus particles toward other cells late during infection, promoting spread of virus from cell to cell. Doceul et al. (2010) observed that an infected cell can produce two important proteins, called A33 and A36, and express them on the cell's outer membrane shortly after infection, which mark the cell as infected. The two proteins are necessary and sufficient to induce formation of actin tails after binding extracellular enveloped vaccinia (EEV) virus. When other cell-free vaccinia viral particles reach the infected cell and contact with these proteins, they induce the host cell to form a new actin tails projection, which propels viral particles away and toward other cells that they can infect. This way, the superinfection is blocked, and the free particles bounce from one cell surface to another until they reach an uninfected cell. This mechanism accelerates virus spread, since virus spreads by surfing from cell to cell, bouncing past the already infected cells and quickly reaching distant uninfected cells without the need to replicate in each cell on the way.

It is believed that some other viruses may also employ such mechanisms to speed up the spread. For instance, herpes simplex virus (HSV-1), which has replication kinetics similar to vaccinia virus, also spreads faster than predicted by their replication kinetics. Considering this repulsion effect of infected cells on superinfecting virions, we see that the spread rate of viruses should depend on the density of infected cells, and high density of infected cells should promote the spread of viruses. We wish to explore this effect quantitatively by mathematical models.

Mathematical modeling has been shown to be an effective and valuable approach to understand the within-host dynamics of virus infection and spread. The dynamics of HIV-1, hepatitis B virus (HBV) and human T-cell leukemia type-1 (HTLV-1) infections have been analyzed in detail with the help of mathematical models. Most of these works are based on the assumption that cells and viruses are well mixed, and hence, ignore the mobility of cells and viruses. However, spatial structure is very important for virus dynamics. In the study of evolutionary competitiveness of lytic virus, Komarova (2007) considered the spatial dynamics of viral spread by a diffusion model and found that lytic viruses can be evolutionary competitive due to the mechanism that they exit an infected cell in a large burst such that the antibodies are flooded and a large proportion of virions can escape the immune system and spread to new cells. The efficacy of the flooding depends on the diffusion rate of the antibodies. Wang and Wang (2007) developed a reaction diffusion model to simulate the infection and spread of HBV. They assumed that susceptible host cells and infected cells cannot move, while viruses move according to Fickian diffusion. For this model, they discussed existence

of traveling wave solutions and minimal wave speed. In a subsequent paper, Gan et al. (2010) considered the effect of the time delay accounting for the lag from the time of infection to the time when the infected cell becomes productively infectious. Xu and Ma (2009) considered the saturation response of the infection rate.

In this paper, we consider the repulsion effect of infected cells on the spread of virus in the within-host environment. Denoting by $T(t, x)$, $I(t, x)$ and $V(t, x)$, the concentrations of target cells, infected cells and free virus particles at time t at location x, respectively, we consider the following general virus infection dynamic model,

$$
\begin{aligned}
\frac{\partial T}{\partial t} &= D_T \Delta T + h(x) - d_T T - \beta(x) T V, \\
\frac{\partial I}{\partial t} &= D_T \Delta I + \beta(x) T V - d_I I, \\
\frac{\partial V}{\partial t} &= \nabla \cdot (D_V(I) \nabla V) + \gamma(x) I - d_V V.
\end{aligned}
\tag{1}
$$

This model system is based on some assumptions. Firstly, the within-host environment is spatially heterogenous, that is, the target cell production rate $h(x)$, infection rate $\beta(x)$ and free virus production rate $\gamma(x)$ may depend on the spatial location x. These three functions are assumed to be positive, continuous and bounded. The death rates of target cells, infected cells and viruses are constants, denoted by d_T, d_I and d_V, respectively. Secondly, target cells and infected cells can move, following the Fickian diffusion, meaning that the fluxes of these cells are proportional to their concentration gradient and go from regions of high concentration to regions of low concentration, with the same diffusion rate D_T, that is,

$$
\vec{J}_T = -D_T \nabla T, \quad \vec{J}_I = -D_T \nabla I.
$$

Notice that the diffusion rate of the cells may be much slower in contrast to the spreading rate of viruses and is thus often neglected in literature. Thirdly, the flux of free viral particles depends not only on its concentration gradient but also on the concentration of infected cell in the following form

$$
\vec{J}_V = D_V(I)(-\nabla V).
$$

The repulsion of the superinfecting virions observed in (Doceul et al. 2010) suggests that high concentration of infected cells promotes spread of viruses toward uninfected target cells. Therefore, $D_V(I)$ should be an increasing function of the local concentration of infected cells $I(t, x)$. We assume

$$
D_V(I) = D_0 + g(I),
$$

where D_0 represents random diffusion rate of free virions and $g \in \mathbf{C}^2(\mathbb{R}_+, \mathbb{R}_+)$ is an increasing function of I, representing the motility of free virions due to repulsion of superinfecting virions by infected cells. If there is no infected cell, then there is no repulsion effect, meaning that $g(I)$ should satisfy $g(0) = 0$.

The rest of the paper is organized as follows. In Sect. 2, we discuss the well posedness of the model (1), derive the basic reproduction number $\mathcal{R}_0$ of the system (1) and calculate $\mathcal{R}_0$ numerically. For the model (1), mathematical proof of stability of steady states is difficult to approach. However, when all the parameters $h(x)$, $\beta(x)$ and $\gamma(x)$ do not depend on space location x, we can establish the linear stability of steady states of system (1). In Sect. 3, we numerically estimate the spreading rate of virus and discuss the effect of repulsion of superinfecting virions. Section 4 discusses existence of traveling wavefront solutions to the model and their numerical simulations when the diffusion of target cells and infected cells is ignored. Finally, we present conclusions and discussion in Sect. 5.

2 Dynamics in a Bounded Domain

In this section, we consider an open-bounded domain $\Omega \subset \mathcal{R}^3$ with smooth boundary $\partial \Omega$. Under such a scenario, we examine the dynamics of the model. More precisely, we will investigate the dynamics of the system

$$
\begin{aligned}
\frac{\partial T}{\partial t} &= D_T \Delta T + h(x) - d_T T - \beta(x) T V, \\
\frac{\partial I}{\partial t} &= D_T \Delta I + \beta(x) T V - d_I I, \qquad x \in \Omega, \ t > 0, \\
\frac{\partial V}{\partial t} &= \nabla \cdot (D_V(I) \nabla V) + \gamma(x) I - d_V V,
\end{aligned} \tag{2}
$$

with zero-flux boundary conditions

$$
\frac{\partial T}{\partial \nu} = \frac{\partial I}{\partial \nu} = \frac{\partial V}{\partial \nu} = 0, \ \forall x \in \partial \Omega, \ t > 0, \tag{3}
$$

and initial conditions

$$
T(0, x) = T_0(x) > 0, \ \ I(0, x) = I_0(x) \geq 0, \ \ V(0, x) = V_0(x) \geq 0, \ \ \forall x \in \Omega. \tag{4}
$$

2.1 Well Posedness of the Model

First, we address the well posedness of the problem (2)–(4). As usual, we denote by $\mathbb{R}_+^3$ the positive cone in $\mathbb{R}^3$, i.e.,

$$
\mathbb{R}_+^3 = \left\{ w = (T, I, V)^{\mathrm{T}} \in \mathbb{R}^3 \mid T \geq 0, I \geq 0, V \geq 0 \right\},
$$

Let $p > 3$ so that the space $\mathbf{W}^{1,p}(\Omega, \mathbb{R}^3)$ is continuously embedded in the continuous function space $\mathbf{C}(\Omega, \mathbb{R}^3)$ (see, e.g., Adams 1975). Since the unknowns T, I and V are populations, we only need to consider the following phase space:

$$\mathbf{X}_+ := \left\{ w \in \mathbf{W}^{1,p}(\Omega, \mathbb{R}^3) \mid w(\bar{\Omega}) \subset \mathbb{R}_+^3 \ \text{and} \ \frac{\partial w}{\partial \nu} = 0 \ \text{on} \ \partial\Omega \right\}.$$

We see that the system (2)–(3) can be rewritten as the following abstract quasi-linear parabolic system

$$\begin{cases} w_t + \mathcal{A}(w)w = \mathcal{F}(x, w), & x \in \Omega, \ t > 0, \\ \mathcal{B}w = 0, \ x \in \partial\Omega, \ t > 0, \end{cases} \tag{5}$$

where

$$\mathcal{A}(z)w = -\sum_{j,k} \partial_j(a_{jk}(z)\partial_k w), \quad \mathcal{B}w = \frac{\partial w}{\partial \nu},$$

and

$$a_{jk} = a(z)\delta_{jk}, \quad 1 \le j, k \le 3, \quad a(z) = \begin{pmatrix} D_T & 0 & 0 \\ 0 & D_T & 0 \\ 0 & 0 & D_V(z_3) \end{pmatrix},$$

for $z = (z_1, z_2, z_3) \in \mathbb{R}_+^3$ (here δ_{jk} is the Kronecker delta function), and

$$\mathcal{F}(x, w) = (h(x) - d_T T - \beta(x)TV, \beta(x)TV - d_I I, \gamma(x)I - d_V V)^\mathsf{T},$$

for $w = (T, I, V)$. It is obvious that $a(z) \in \mathbf{C}^2(\mathbb{R}_+^3, \mathcal{L}(\mathbb{R}_+^3))$, where we identified $\mathcal{L}(\mathbb{R}_+^3)$ with the space of 3×3 real matrices. Since $D_V(I) \ge D_0 > 0$, the eigenvalues of $a(z)$ are positive for each $z \in \mathbb{R}_+^3$. Moreover, the boundary value problem $(\mathcal{A}, \mathcal{B})$ is normally elliptic (see, e.g., Amann 1993).

For the global existence and nonnegativity of solutions, we have the following theorem.

Theorem 2.1 *For every initial data* (T_0, I_0, V_0), *(2)–(3)–(4) has a unique solution defined on* $[0, \infty) \times \Omega$, *such that*

$$(T, I, V) \in \mathbf{C}([0, \infty), \mathbf{X}_+) \cap \mathbf{C}^{2,1}((0, \infty) \times \bar{\Omega}, \mathbb{R}^3).$$

Moreover, the solution satisfies $T(t, x) \ge 0$, $I(t, x) \ge 0$, $V(t, x) \ge 0$, *for all* $(t, x) \in [0, \infty) \times \Omega$.

Proof See "Appendix 1".   □

2.2 Basic Reproduction Number

Let $\mathbb{X} := \mathbf{C}(\bar{\Omega}, \mathbb{R}^3)$ be the Banach space of continuous functions with supremum norm $\|\cdot\|_\mathbb{X}$. Denote by $\mathbb{X}_+$ the positive cone of $\mathbb{X}$, i.e., $\mathbb{X}_+ = \mathbf{C}(\bar{\Omega}, \mathbb{R}_+^3)$. Then, $\mathbb{X}_+$ induces a partial order, making $(\mathbb{X}, \mathbb{X}_+)$ strongly ordered space. Similarly, let $\mathbb{Y} := \mathbf{C}(\bar{\Omega}, \mathbb{R})$ and $\mathbb{Y}_+ := \mathbf{C}(\bar{\Omega}, \mathbb{R}_+)$. Suppose that for each $t \ge 0$, $S_1(t)$ and $S_2(t) : \mathbb{Y} \to \mathbb{Y}$ are the

strongly continuous semigroups associated with $D_T \Delta - d_I$ and $D_0 \Delta - d_V$ subject to homogeneous Neumann boundary conditions, respectively, that is,

$$[S_1(t)\phi](x) = e^{-d_I t} \int_\Omega \Gamma(x, y, t, D_T)\phi(y)dy,$$

$$[S_2(t)\phi](x) = e^{-d_V t} \int_\Omega \Gamma(x, y, t, D_0)\phi(y)dy,$$

for any $\phi_1, \phi_2 \in \mathbb{Y}$, $t \geqslant 0$, where $\Gamma(x, y, t, D_T)$ and $\Gamma(x, y, t, D_0)$ are the Green functions associated with $D_T \Delta$ and $D_0 \Delta$ subject to homogenous Neumann boundary conditions, respectively. It then follows that for each $t > 0$, $S_i(t) : \mathbb{Y} \to \mathbb{Y}$, $i = 1, 2$ is compact and strongly positive (Smith 1995, Corollary 7.2.3). Therefore, $S(t) = (S_1(t), S_2(t))$ is a positive C_0-semigroup.

Setting $I(t, x) = 0$ and $V(t, x) = 0$ in the T equation in (2) leads to

$$\frac{\partial T(t, x)}{\partial t} = D_T \Delta T(t, x) + h(x) - d_T T(t, x), \quad x \in \Omega, \ t > 0,$$
$$\frac{\partial T(t, x)}{\partial \nu} = 0, \quad x \in \partial\Omega, \ t > 0. \tag{6}$$

From Lemma 1 in Lou and Zhao (2011), we know (6) admits a unique positive steady state $\hat{T}(x)$, which is globally attractive in $\mathbf{C}(\bar{\Omega}, \mathbb{R})$. This means that the model system (2) has a unique infection-free steady state $E_0 = (\hat{T}(x), 0, 0)$.

Linearizing (2) at the infection-free steady state E_0, we obtain the linearized system

$$\frac{\partial u_1}{\partial t} = D_T \Delta u_1 - d_T u_1 - \beta(x)\hat{T}(x)u_3,$$
$$\frac{\partial u_2}{\partial t} = D_T \Delta u_2 + \beta(x)\bar{T}(x)u_3 - d_I u_2,$$
$$\frac{\partial u_3}{\partial t} = D_0 \Delta u_3 + \gamma(x)u_2 - d_V u_3, \tag{7}$$

subject to the boundary conditions

$$\frac{\partial u_1}{\partial \nu} = \frac{\partial u_2}{\partial \nu} = \frac{\partial u_3}{\partial \nu} = 0, \quad \forall x \in \partial\Omega, \ t > 0.$$

We see that the equations for u_2 and u_3, which correspond to the infectious compartments, are decoupled from u_1, and these two equations constitute a cooperative system. Substituting $u_2(x, t) = e^{\lambda t}\phi_1(x)$ and $u_3(x, t) = e^{\lambda t}\phi_2(x)$ into equations of u_2 and u_3, we obtain the following eigenvalue problem

$$\lambda\phi_1(x) = D_T \Delta\phi_1(x) + \beta(x)\hat{T}(x)\phi_2(x) - d_I\phi_1(x),$$
$$\lambda\phi_2(x) = D_0 \Delta\phi_2(x) + \gamma(x)\phi_1(x) - d_V\phi_2(x), \tag{8}$$

$$\frac{\partial \phi_1(x)}{\partial v} = \frac{\partial \phi_2(x)}{\partial v} = 0, \quad \forall x \in \partial \Omega, \ t > 0,$$

where $\phi = (\phi_1, \phi_2) \in \mathbb{Y} \times \mathbb{Y}$.

From Theorem 7.6.1 in Smith (1995), we have the following result.

Lemma 2.1 *The eigenvalue problem* (8) *has a principal eigenvalue* $\lambda_0(D_0, D_T, \hat{T}(x))$ *associated with a strictly positive eigenvector.*

This means that λ_0 is a real eigenvalue with algebraic multiplicity one, and $Re(\lambda) < \lambda_0$ for any other eigenvalue λ of (8). Furthermore, λ_0 has a corresponding eigenvector $\phi_0(x) = (\phi_{01}, \phi_{02})$ satisfying $\phi_0(x) \gg 0$, and any other nonnegative eigenvector of (8) is a positive multiple of $\phi_0(x)$.

Next, as in Wang and Zhao (2011), Guo et al. (2012) and Vaidya et al. (2012), we follow the framework of Thieme (2009) to obtain the basic reproduction number of the model (2). To this end, we define a positive linear operator by

$$C(\phi)(x) = (C_1(\phi)(x), C_2(\phi)(x)), \quad \forall \phi = (\phi_1, \phi_2) \in \mathbb{Y} \times \mathbb{Y}, \ x \in \bar{\Omega},$$

where

$$C_1(\phi)(x) = \beta(x)\hat{T}(x)\phi_2(x), \ C_2(\phi)(x) = \gamma(x)\phi_1(x).$$

Assume that there are no infected cells and free virus initially, that is, the system is near the infection-free steady state; and viruses are introduced at time $t = 0$ and infection occurs immediately. The distribution of initial infected cells and free viruses is assumed to be $(\phi_1(x), \phi_2(x))$ (at time $t = 0$). Then, as time evolves, those distributions reach $([S_1(t)\phi_1](x), [S_2(t)\phi_2](x))$ at time t. Thus, the total distribution of new infected cells is

$$\int_0^\infty \beta(x)\hat{T}(x)[S_2(t)\phi_2](x)\mathrm{d}t = \left[\int_0^\infty C_1(S(t)\phi)\mathrm{d}t\right](x),$$

and the total distribution of new free viruses is

$$\int_0^\infty \gamma(x)[S_1(t)\phi_1](x)\mathrm{d}t = \left[\int_0^\infty C_2(S(t)\phi)\mathrm{d}t\right](x).$$

Therefore, the next generation operator L is given by

$$L(\phi) := \int_0^\infty C(S(t)\phi)\mathrm{d}t = C\left(\int_0^\infty S(t)\phi\mathrm{d}t\right).$$

The basic reproduction number of the model (2) is defined to be the spectral radius of L, that is,

$$\mathcal{R}_0 := r(L).$$

We point out that the above procedure of defining the basic reproduction number for reaction–diffusion systems has recently been standardized in Wang and Zhao (2012). By Theorem 3.1 (i) in Wang and Zhao (2012), we then obtain the following Lemma.

Lemma 2.2 $\mathcal{R}_0 - 1$ *has the same sign as* λ_0.

When all parameters are location independent (spatially homogeneous), we can actually find an explicit formula for the basic reproduction number $\mathcal{R}_0$. Indeed, applying Theorem 3.4 in Wang and Zhao (2012) and similar arguments to the proof of Theorem 2.3 in Wang and Zhao (2011), we obtain the following theorem.

Theorem 2.2 *Assume that* $\beta(x)$, $\gamma(x)$ *and* $h(x)$ *are positive constants, so that* $\hat{T}(x)$ $= \frac{h}{d_T}$. *Then*

$$\mathcal{R}_0 = \sqrt{\frac{\beta h \gamma}{d_T d_V d_I}}.$$

Remark 2.1 Note that, here, we define the basic reproduction number as the spectral radius of the next generation operator/matrix (Thieme 2009; Wang and Zhao 2011, 2012), which gives the mean number of new infections per infective in any class of infected cell population and virus population, per generation. However, in another way, the basic reproduction number is defined as the total number of newly infected cells (or viral particles) produced by one infected cell (or virus) during its lifetime, assuming all other target cells are susceptible (Heffernan et al. 2005). By this definition, we have the basic reproduction number

$$\mathcal{R}_0 = \frac{\beta h \gamma}{d_T d_V d_I},$$

for the case when all parameters are constants. The dynamics of the model are always determined by whether or not $\mathcal{R}_0$ exceeds 1. Thus, these two definitions of the basic reproduction number will not affect the dynamics of the model. In general, the former definition is widely used in the biomathematics literature, while the latter definition is extensively used in epidemiology and immunology (see Heffernan et al. 2005 and references therein).

For spatial heterogeneous case, that is, if at least one of the model parameters $h(x)$, $\beta(x)$ and $\gamma(x)$ depends on the space location x, we cannot derive an explicit formula for $\mathcal{R}_0 = r(L)$. However, we can compute the spectral radius of the linear operator L numerically by using the orthogonal projection method in computation of eigenvalues for compact linear operators (Chatelin 1981). For the sake of convenience, we consider $\Omega = (0, 1)$ to demonstrate this numerical method. We use nth-order Fourier projection (Ikebe 1972), where the orthonormal basis is assumed to be $e_k(x)$ $= \mathrm{e}^{2k\pi x i}$, $k \in \mathbb{N}$, and then use the Galerkin method. For $\Omega = (0, 1)$, the Green function associated with $D\Delta$, subject to homogenous Neumann Boundary condition, assumes the following explicit form (Haberman 1998)

$$\Gamma(x, y, t, D) = 1 + 2 \sum_{n=1}^{\infty} e^{-Dn^2\pi^2 t} \cos(n\pi x) \cos(n\pi y).$$

For the operator L, the Galerkin matrix is

$$B_n = \begin{pmatrix} 0 & A_n^{(1)} \\ A_n^{(2)} & 0 \end{pmatrix},$$

where

$$A_n^{(1)} = \left(a_{jk}^{(1)}\right)_{n \times n}, \quad A_n^{(2)} = \left(a_{jk}^{(2)}\right)_{n \times n}.$$

Here,

$$a_{jk}^{(1)} = \int_0^1 \overline{e_j(x)} \int_0^1 K_1(x, y) e_k(y) \mathrm{d}y \mathrm{d}x, \quad a_{jk}^{(2)} = \int_0^1 \overline{e_j(x)} \int_0^1 K_2(x, y) e_k(y) \mathrm{d}y \mathrm{d}x.$$

Then, we have

$$K_1(x, y) = \beta(x)\hat{T}(x) \left[\frac{1}{d_V} + 2 \sum_{n=1}^{\infty} \frac{1}{D_0 n^2\pi^2 + d_V} \cos(n\pi x) \cos(n\pi y) \right],$$

$$K_2(x, y) = \gamma \left[\frac{1}{d_I} + 2 \sum_{n=1}^{\infty} \frac{1}{D_T n^2\pi^2 + d_I} \cos(n\pi x) \cos(n\pi y) \right].$$

Wang and Zhao (2012) offered an alternative method of numerically computing basic reproduction number $\mathcal{R}_0$ by numerically computing the unique positive eigenvalue of an elliptic eigenvalue problem (Wang and Zhao 2012). Indeed, by Theorem 3.2 in Wang and Zhao (2012), $\mathcal{R}_0$ is given by the reciprocal of the unique positive eigenvalue of the following eigenvalue problem

$$-D\triangle\phi + V(x)\phi = \mu F(x)\phi, \quad x \in \Omega,$$
$$\frac{\partial \phi}{\partial \nu} = 0, \quad x \in \partial\Omega. \tag{9}$$

Using the method developed in Wang and Zhao (2012), we can also numerically calculate the basic reproduction number.

Figures 1 and 2 are the plots of the numeric computations of the spectral radius of L with the following baseline parameters

$$h = 10^5, \quad d_T = 0.1, \quad d_I = 0.1, \quad d_V = 5, \quad \gamma = 500, \quad \beta(x) = 5 \times 10^{-10} x^2,$$

showing how the basic reproduction number $\mathcal{R}_0$ depends on the diffusion rate of infected cells D_T, the basic diffusion rate of free virus D_0, and virus production rate
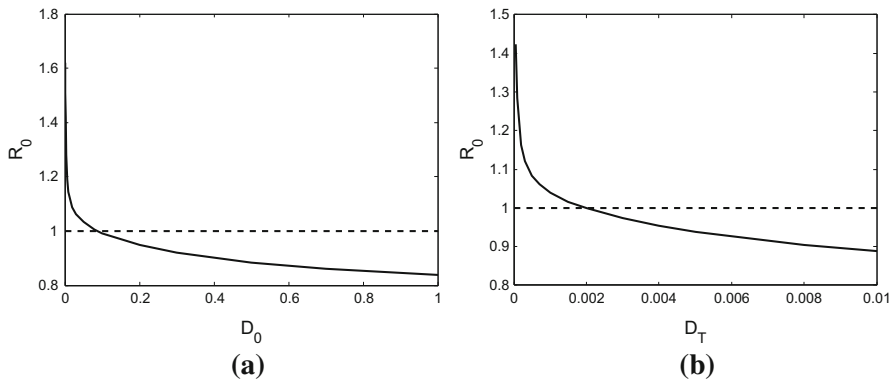
Fig. 1 Basic reproduction number $\mathcal{R}_0$ is a decreasing function of D_0 and D_T, where **a** $D_T = 0.00001$, and **b** $D_0 = 0.0001$
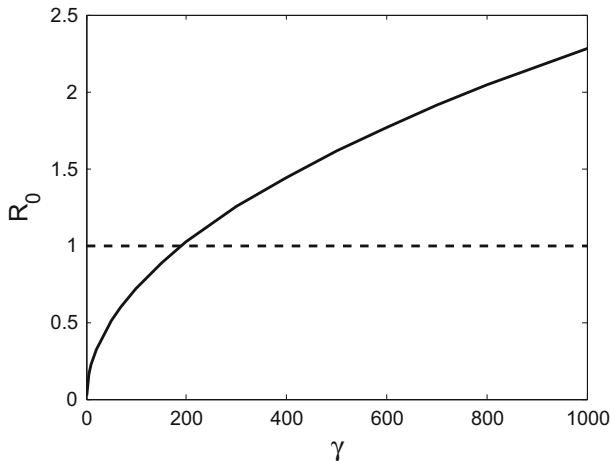

Fig. 2 Basic reproduction number $\mathcal{R}_0$ is an increasing function of γ. Here $D_0 = 0.0001$, $D_T = 0.00001$

γ, respectively. Note that in the spatially homogeneous case, the diffusion coefficients have no impact on $\mathcal{R}_0$.

2.3 Steady States and Their Linear Stability

For the model (2)–(3)–(4), by the biological meaning of the basic reproduction number $\mathcal{R}_0$, it is expected that the infection-free steady state $E_0 = (\bar{T}(x), 0, 0)$ is asymptotically stable if $\mathcal{R}_0 < 1$, and there should exist a positive steady state if $\mathcal{R}_0 > 1$.

By the proof of Theorem 3.1 (ii) in Wang and Zhao (2012), we have the following stability/instability results for E_0:

Lemma 2.3 *If $\mathcal{R}_0 < 1$, then E_0 is linearly stable; if $\mathcal{R}_0 > 1$, then E_0 is linearly unstable, regardless of whether or not the model parameters are spatially dependent.*

Since the equations of $u_2(t)$ and $u_3(t)$ in (7) are decoupled from the $u_1(t)$ equation, it follows that if $\mathcal{R}_0 > 1$, then E_0 is linearly unstable. However, when the model parameters are spatially dependent, it is mathematically difficult to prove the existence of positive steady state. In the rest of the paper, we only focus on the case when $h(x)$, $\beta(x)$ and $\gamma(x)$ are all positive constants. For the following spatial homogeneous model,

$$
\begin{aligned}
\frac{\partial T}{\partial t} &= D_T \Delta T + h - d_T T - \beta T V, \\
\frac{\partial I}{\partial t} &= D_T \Delta I + \beta T V - d_I I, \qquad x \in \Omega, \ \ t > 0, \qquad (10) \\
\frac{\partial V}{\partial t} &= \nabla \cdot (D_V(I)\nabla V) + \gamma I - d_V V,
\end{aligned}
$$

in addition to the infection-free steady state $E_0 = (h/d_T, 0, 0)$, it also has a positive steady state $\bar{E} = (\bar{T}, \bar{I}, \bar{V})$ whenever $\mathcal{R}_0 > 1$, where

$$
\bar{T} = \frac{h}{d_T \mathcal{R}_0^2}, \quad \bar{I} = \frac{d_T d_V}{\beta \gamma}\left(\mathcal{R}_0^2 - 1\right), \quad \bar{V} = \frac{d_T}{\beta}\left(\mathcal{R}_0^2 - 1\right).
$$

Here, $\mathcal{R}_0$ is the basic reproduction number of (2) with $h, \ \gamma$ and β being constants, which has been determined before, that is,

$$
\mathcal{R}_0^2 = \frac{\beta h \gamma}{d_T d_V d_I}.
$$

Note that E_0 and $\bar{E}$ (if $\mathcal{R}_0 < 1$) are also the steady states in the absence of spatial diffusions, and in such case, it has been shown in (Korobeinikov 2004) that E_0 is globally asymptotically stable if $\mathcal{R}_0 \leq 1$; $\bar{E}$ is globally asymptotically stable if $\mathcal{R}_0 > 1$. For the model (2) with diffusions and with no-flux boundary condition, we have the following results on the linear stability of $\bar{E}$.

Theorem 2.3 *For (10), the positive steady state $\bar{E}$ is linearly stable if it exists.*

Proof See "Appendix 1". □

3 Spreading Speed in the Case $\Omega = \mathbb{R}$

In the above section, we have seen that in a bounded domain setting, the repulsion effect of infected cells does not change the threshold dynamics characterized by $\mathcal{R}_0$. Note that it has been observed in the experiment (Doceul et al. 2010) that the repulsion effect accelerates the spreading rate of viruses across cells. In this section, we use the model (1) to quantitatively investigate the spreading rate of the virus and see how the repulsion effect will affect the spreading speed. Unfortunately, due to the dependence of $D_V(I)$ on I, to the author's knowledge, the existing theories for spreading speed do not apply to (1). While a new theory needs to be developed, we will explore this topic numerically here. As in most studies on this topic, we consider the domain $\Omega = \mathbb{R}$ for the spatial variable x, mainly for the convenience in discussing this topic.
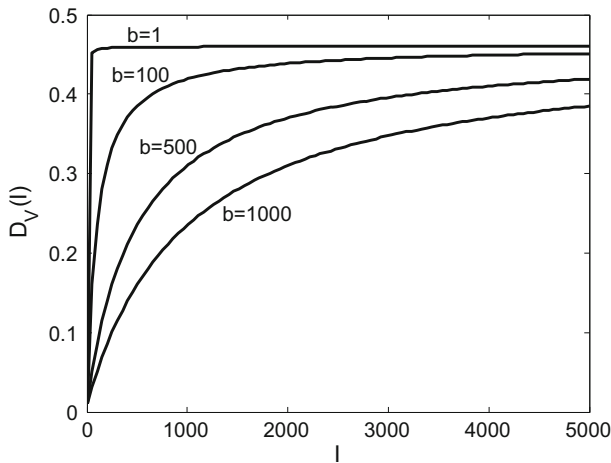
Fig. 3 Diffusion function of virus $D_V(I) = D_0 + aI/(b+I)$, where we take $D_0 = 0.01$, $a = 0.45$

To proceed, we choose the following particular function for the diffusion of free virus:

$$D_V(I) = D_0 + \frac{aI}{b+I}. \tag{11}$$

Here, the repulsion effect is characterized by $g(I) = \frac{aI}{b+I}$, which satisfies $g(0) = 0$, and is an increasing function of I. The parameter a indicates the saturation level and b describes how quickly $g(I)$ increases to its saturation level (see Fig. 3). Since our focus is on the repulsion effect, for convenience, here, we neglect the mobility of target cells (both infected and uninfected).

That is, we assume $D_T = 0$ and consider the following model:

$$\begin{aligned}
\frac{\partial T}{\partial t} &= h - d_T T - \beta T V, \\
\frac{\partial I}{\partial t} &= \beta T V - d_I I, \qquad t > 0, \\
\frac{\partial V}{\partial t} &= \nabla \cdot (D_V(I)\nabla V) + \gamma I - d_V V.
\end{aligned} \tag{12}$$

The baseline parameter values are taken from Bonhoeffer et al. (1997) as follows: $h = 10^7$, $\beta = 5 \times 10^{-10}$, $\gamma = 500$, $T = 0.1$, $d_V = 5$, $d_I = 0.1$, $D_0 = 0.0001$ and $b = 1$. In this case, the basic reproduction number is $\mathcal{R}_0 = \sqrt{50}$, and the positive steady state is $(\bar{T}, \bar{I}, \bar{V}) = (0.2 \times 10^7, 9.8 \times 10^7, 9.8 \times 10^9)$.

We consider different initial distribution functions $T_0(x)$, $I_0(x)$ and $V_0(x)$, and observe, by numerical simulations, the evolution of virus population. First, when the initial distributions assume

$$T_0(x) = 10^7, \quad I_0(x) = 0, \quad V_0(x) = \begin{cases} 0 & x < 0 \\ 100 & x = 0, \\ 0 & x > 0 \end{cases}$$
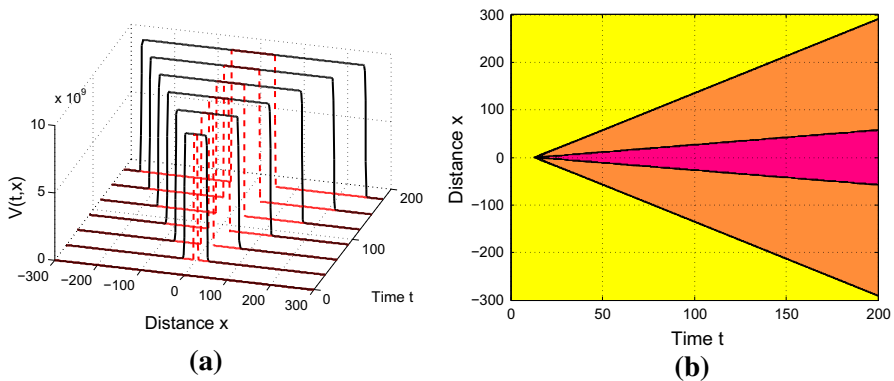
Fig. 4 **a** Evolution of $V(t, x)$ from the initial distribution $V_0(x)$, where *dashed line red*: $a = 0$, *solid line black*: $a = 0.45$. **b** The contour of (**a**) (Color figure online)

meaning that 100 viruses are initially innoculated at the location $x = 0$. Numerical results are plotted in Fig. 4a for $a = 0$ (no repulsion effect) and $a = 0.45$ (with repulsion effect). From the numerical results, we can estimate the asymptotic spreading speed using the method described by Neubert and Parker (2004). More precisely, we assume there is some threshold for virus population density $\tilde{V}$ below which we cannot detect the presence of the virus population. Let $\tilde{x}(t)$ be the location where the population density equals $\tilde{V}$. The asymptotic spreading speed is defined as the rate of increase of $\tilde{x}(t)$ as t increases, that is, $c = \lim_{t \to \infty} \frac{d\tilde{x}(t)}{dt}$. This is an average speed at which the population propagates finally. The slope of boundaries of inner (outer) triangle region in Fig. 4b is the asymptotic spreading speed of free virus population in the absence (presence) of repulsion effect.

Taking $\tilde{V} = 0.1$, we see from Fig. 4b that when there is no repulsion effect ($a = 0$), the spreading speed of virus is approximately equal to $c = 0.304$, while in the presence of repulsion effect ($a > 0$), virus spreads more quickly: for $a = 0.45$, the spreading speed is approximately $c = 1.547$, which is more than five times quickly than the spreading speed without repulsion effect. This is in close agreement with experimental results observed in Doceul's experiment (Doceul et al. 2010). Indeed, it was observed (Doceul et al. 2010) that vaccinia virus spreads across one cell every 1.2 h, but in vaccinia replication kinetics, new virions are formed only 5–6 h after infection (or, by virus-induced cell motility, cell starts to move 5–6 h after infection). In other words, the vaccinia virus spreads across one cell more faster than thought the rate at which it replicates (1.2 vs 5–6 h). As pointed out in Condit (2010), Doceul et al. (2010) and confirmed by our model simulations, such a faster spreading speed is attributed to repulsion effect of superinfecting virions by infected cells.

For different initial distributions, the virus population also spreads at the same speed as $c = 0.304$ for the case without repulsion effect and $c = 1.547$ for the case with repulsion effect. Figure 5 gives the numeric simulation results on the evolution of virus population described by the model (12) for the following initial distribution,

$$T_0(x) = 10^7, \quad I_0(x) = 0, \quad V_0(x) = \begin{cases} 0 & x \leq -6\pi \\ 50(1 + \cos(x/\pi)) & -6\pi < x \leq 6\pi \\ 0 & x > 6\pi \end{cases}.$$
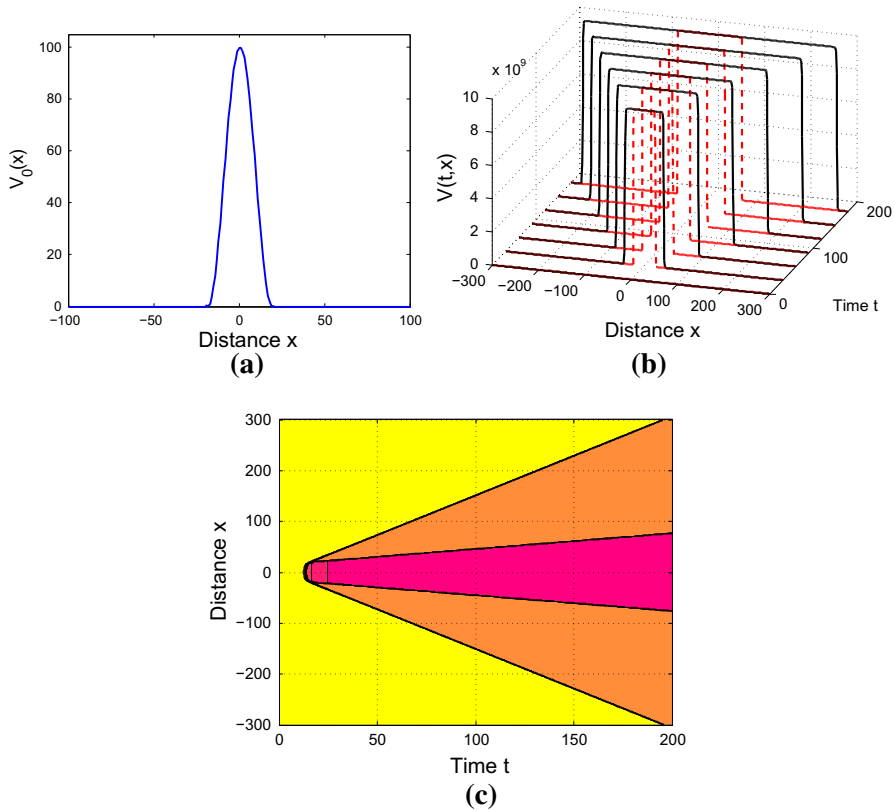
Fig. 5 **a** Initial distribution $V_0(x)$. **b** The evolution of $V(t, x)$ from the initial distribution, where *dashed line (red)*: $a = 0$, *solid line (black)*: $a = 0.45$. **c** The contour of (**b**) (Color figure online)

4 Existence of Traveling Wave Solutions in the Case $\Omega = \mathbb{R}$

Traveling wavefront solutions are a class of solutions which are in a particular form incorporating the time variable and spatial variable through a moving coordinate. Such a solution describes the spatial transition from one steady state to another. For traveling wavefronts connecting an unstable steady state and a stable steady state, typically, there is a minimal wave speed, which is closely related to the spreading speed discussed in the preceding section. Indeed, there have been many works confirming that in many model systems, the two speeds coincide (mainly monotone systems), while there are also model systems in which the two speeds are different (see, e.g., Li et al. 2005; Lewis et al. 2002).

In this section, we will explore the existence of traveling wavefront connecting the infection-free steady state E_0 and the infection steady state $\bar{E}$, all under the same assumptions/scenario as in the preceding section. That is, we still consider the case $\Omega = \mathbb{R}$ and assume that target cells and infected cells do not move, while viral particles diffuse, and consider the following model

$$\frac{\partial T}{\partial t} = h - d_T T - \beta T V,$$
$$\frac{\partial I}{\partial t} = \beta T V - d_I I, \tag{13}$$
$$\frac{\partial V}{\partial t} = \nabla \cdot (D_V(I)\nabla V) + \gamma I - d_V V.$$

Rescaling the model (13) by

$$\tilde{t} = d_T t, \ \tilde{x} = x,$$
$$u = (d_T/h)T, \ w = (d_T/h)I, \ v = (\beta/d_T)V,$$
$$\rho_1 = d_I/d_T, \ \rho_2 = \gamma\beta h/d_T^3, \ \rho_3 = d_V/d_T,$$
$$D(w) = D_V(h/d_T w)/d_T,$$

we obtain (dropping the tildes on t and x)

$$\frac{\partial u}{\partial t} = 1 - u - uv,$$
$$\frac{\partial w}{\partial t} = uv - \rho_1 w, \tag{14}$$
$$\frac{\partial v}{\partial t} = \nabla \cdot (D(w)\nabla v) + \rho_2 w - \rho_3 v.$$

This rescaled system has two steady states $E_0 = (1, 0, 0)$ and $\bar{E} = (\bar{u}, \bar{w}, \bar{v})$ where

$$\bar{u} = \frac{\rho_1 \rho_3}{\rho_2}, \ \bar{w} = \frac{\rho_2 - \rho_1 \rho_3}{\rho_1 \rho_2}, \ \bar{v} = \frac{\rho_2 - \rho_1 \rho_3}{\rho_1 \rho_3}.$$

Obviously, E_0 and $\bar{E}$ are just result of rescaling E_0 and $\bar{E}$ in preceding sections, and $\bar{E}$ is biologically meaningful (positive) iff $\rho_2 > \rho_1 \rho_3$ which is equivalent to $\mathcal{R}_0 = \sqrt{\gamma\beta h/d_T d_I d_V} = \sqrt{\rho_2/\rho_1 \rho_3} > 1$.

Traveling wave solutions of (14) are solutions of the form $\tilde{u}(x, t) = u(x + ct)$, $\tilde{w}(x, t) = w(x + ct)$, $\tilde{v}(x, t) = v(x + ct)$ where $c > 0$ represents the speed of traveling wave solutions. Substituting this solution form into (14), we obtain

$$cu' = 1 - u - uv,$$
$$cw' = uv - \rho_1 w, \tag{15}$$
$$cv' = D'(w)w'v' + D(w)v'' + \rho_2 w - \rho_3 v,$$

where prime denotes differentiation with respect to the wave variable $s = x + ct$.

Letting $z = v'$, system (15) is rewritten as

$$u' = \frac{1}{c}(1 - u - uv),$$
$$w' = \frac{1}{c}(uv - \rho_1 w),$$

$$v' = z,$$

$$z' = \frac{1}{D(w)} \left[cz - \frac{1}{c} D'(w)(uv - \rho_1 w)z - \rho_2 w + \rho_3 v \right], \tag{16}$$

which has two steady states $E_0' = (1, 0, 0, 0)$ and $E_1' = (\bar{u}, \bar{w}, \bar{v}, 0)$ when $\mathcal{R}_0 > 1$. We consider the existence of solutions of (15) satisfying the asymptotic boundary conditions

$$\lim_{s \to -\infty} (u(s), w(s), v(s), z(s)) = (1, 0, 0, 0),$$

$$\lim_{s \to \infty} (u(s), w(s), v(s), z(s)) = (\bar{u}, \bar{w}, \bar{v}, 0), \tag{17}$$

which accounts for transition from the infection-free steady state E_0 to the infection steady state $\bar{E}$.

Behaviors of solutions of (16) near E_0' are typically determined by the linearization of (16) at E_0'. By analyzing this linearization and taking into consideration the feature of traveling wave solutions (see "Appendix 2"), we obtain that system (14) does not have any traveling wavefront solution for $0 < c < c^*$. Here, c^* is determined by the following equation:

$$Q(c) := b_0 c^6 + b_1 c^4 + b_2 c^2 + b_3 = 0, \tag{18}$$

where

$$b_0 = 4\rho_2 + \rho_1^2 + \rho_3^2 - 2\rho_1\rho_3,$$

$$b_1 = D(0) \left(6\rho_2\rho_1 + 2\rho_1^3 - 8\rho_1\rho_3^2 + 4\rho_3^3 + 18\rho_2\rho_3 + 2\rho_1^2\rho_3 \right),$$

$$b_2 = D(0)^2 \left(8\rho_1^3\rho_3 - 8\rho_1^2\rho_3^2 + \rho_1^4 + 36\rho_2\rho_1\rho_3 - 6\rho_2\rho_1^2 - 27\rho_2^2 \right),$$

$$b_3 = 4D(0)^3 \left(\rho_1^4\rho_3 - \rho_2\rho_1^3 \right). \tag{19}$$

Furthermore, c^* satisfies

$$\begin{cases} c^* > \sqrt{D(0)\rho_1} & \text{if } 0 < \rho_1 < \rho_1^*, \\ c^* = \sqrt{D(0)\rho_1} & \text{if } \rho_1 = \rho_1^*, \\ c^* < \sqrt{D(0)\rho_1} & \text{if } \rho_1 > \rho_1^*, \end{cases} \tag{20}$$

where ρ_1^* is determined by

$$\frac{2\sqrt{3}}{9} \sqrt{\rho_1} (\rho_1 + \rho_3)^{3/2} + \rho_1\rho_3 = \rho_2. \tag{21}$$

Although we cannot obtain an explicit formula for c^*, we can numerically calculate it when the model parameters are given. To demonstrate this, we choose the same baseline parameters of (13) as those in the preceding section. Then, for the rescaled
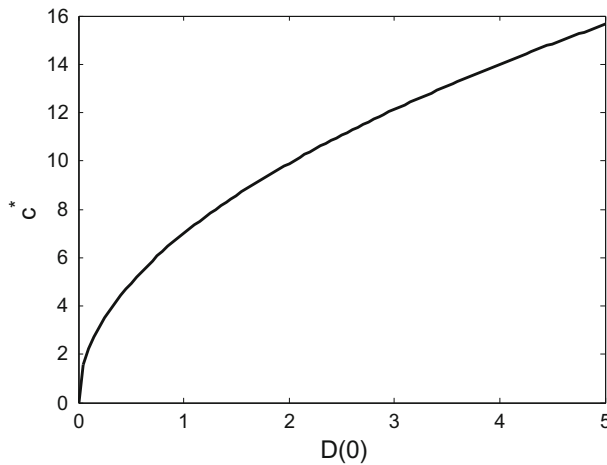
Fig. 6 Impact of $D(0)$ on c^*

model (14), we have $\rho_1 = 1.0$, $\rho_2 = 2500$, $\rho_3 = 50$, $\bar{u} = 0.02$, $\bar{w} = 0.98$, $\bar{v} = 49$. Under the rescaling, the function given in (11) is scaled to

$$D(w) = \frac{1}{d_T}\left(D_0 + \frac{ahw}{d_T b + hw}\right).$$

When $D_0 = 0.0001$ for the original system (13), that is, $D(0) = 0.001$ for the rescaled system (14), numerically solving (18), we obtain $c^* = 0.2214$ for (14). This means that the c^* for original system (13) is $c^* = 0.02214$, since the rescaling is $\tilde{t} = d_T t$, $\tilde{x} = x$ and $d_T = 0.1$. Numerically plotting the solutions of (18) also shows that c^* is an increasing function of $D(0)$, that is, an increasing function of D_0 (see Fig. 6).

We have seen that for $c \in (0, c^*)$, there is no traveling wavefront with speed c that connects E_0 and $\bar{E}$. It is expected that c^* is indeed the minimal wave speed in the sense that for every $c > c^*$, (14) actually has traveling wavefront with speed c that connects E_0 and $\bar{E}$. Unfortunately, we cannot theoretically prove this at the present. In the following, we will explore this numerically. To this end, we use the method developed by Beyn (1990). Firstly, the infinite interval is truncated to a finite interval $[\tau_-, \tau_+]$. Then, we consider the boundary value problem (16) and (17) on this finite interval with additional projection conditions (see Beyn 1990, section 3) and phase conditions (Beyn 1990, section 4). We solve the boundary value problem by BVP solver bvp4c in Matlab. The solutions $y(s) = (u(s), w(s), v(s), z(s))$ are split into two segments, $y_1(s) = (u_1, w_1, v_1, z_1)$ on $[0, \tau_+]$ and $y_2(s) = (u_2, w_2, v_2, z_2)$ on $[0, \tau_-]$, and the interval $[\tau_-, \tau_+]$ is projected onto $[-1, 1]$, such that $y_1(s) = y(s\tau_+)$ and $y_2(s) = y(s\tau_-)$. Thus, we need to consider the following eight-dimensional ODE system,

$$y_1' = \tau_+ f(y_1), \ y_2' = \tau_- f(y_2), \ s \in [0, 1]. \tag{22}$$

We see that $y_1(s)$ and $y_2(s)$ should satisfy the boundary condition

$$y_1(0) = y_2(0). \tag{23}$$

Let ξ_d be an estimate of the derivative $y'(0)$ and ξ_0 be an estimate of $y(0)$. Then, we get the phase condition

$$\xi_d^T(y_1(0) - \xi_0) = 0. \tag{24}$$

Let A_- and A_+ be the Jacobian matrix of (16) at E_0' and E_1', respectively. Let the eigenvectors which span stable subspace of $A_\pm$ be columns of $B_{\pm s}$, the eigenvectors which span unstable subspace of $A_\pm$ be columns of $B_{\pm u}$, and construct

$$B_\pm = (B_{\pm u} B_{\pm s}), \quad B_\pm^{-1} = \begin{pmatrix} L_{\pm u} \\ L_{\pm s} \end{pmatrix},$$

where the rows of $L_{\pm s}$ and $L_{\pm u}$ form a basis for the stable and unstable subspaces of $A_\pm^T$, respectively. The projection conditions are given by

$$L_{+u}(y_1(1) - E_0') = 0, \quad L_{+u}(y_2(1) - E_1') = 0. \tag{25}$$

We solve ODE problem (22) with boundary conditions (23), (24) and (25), by Matlab, where ξ_d and ξ_0 are chosen to be $\xi_d = ((\bar{u} - 1)/2, \bar{w}/2, \bar{v}/2, 0)$ and $\xi_0 = ((\bar{u} + 1)/2, \bar{w}/2, \bar{v}/2, 0)$. The Jacobian of (16) at E_0' is $A_- = J_0$, and that at E_1' is

$$A_+ = \begin{pmatrix} -(1+\bar{v})/c & 0 & -\bar{u}/c & 0 \\ \bar{v}/c & -\rho_1/c & \bar{u}/c & 0 \\ 0 & 0 & 0 & 1 \\ 0 & -\rho_2/D(\bar{w}) & \rho_3/D(\bar{w}) & c/D(\bar{w}) \end{pmatrix}.$$

Setting the parameters as in previous discussions, we can now numerically solve for the traveling wave solutions.

In the absence of repulsion effect, that is $a = 0$, the critical value c^* is obtained by solving the Eq. (18) which is $c^* = 0.02214$. Numerical simulations of the model (14) are given in Figs. 7 and 8. It is seen that for $c < c^*$, $w(s)$ and $v(s)$ go to negative for some values of s, and hence, the system (14) cannot not have traveling wave solution; while for $c > c^*$, traveling wave solution of (14) may exist. For example, $c = 0.23$, the wave profiles of $u(s)$ and $w(s)$ are shown in Fig. 7; $v(s)$ is shown in Fig. 3a. For different values of wave speed c, the traveling wave solutions have different wave profiles. Figure 3b shows the wave profiles of $v(s)$ for $c = 0.23$, $c = 5$ and $c = 10$. In this case, our numerical results show that $c^* = 0.2214$ is indeed that minimal wave speed for system (14), and hence, the minimal wave speed for the original system (13) should be $c^* = 0.02214$ which is much smaller than the spreading speed $c = 0.304$ established in the preceding section.

In the presence of repulsion effect, that is $a > 0$, solving (18) still gives $c^* = 0.2214$ since (18) is independent of a. But our simulations show that this critical value is not minimal wave speed in this case. Fixing $a = 0.45$, from the simulation results shown in
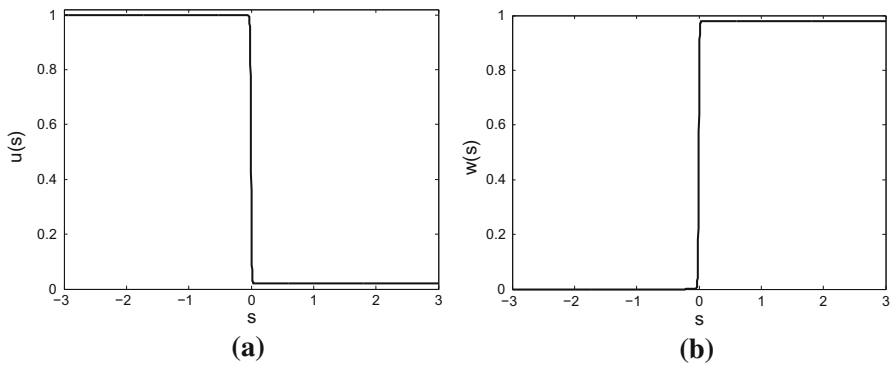
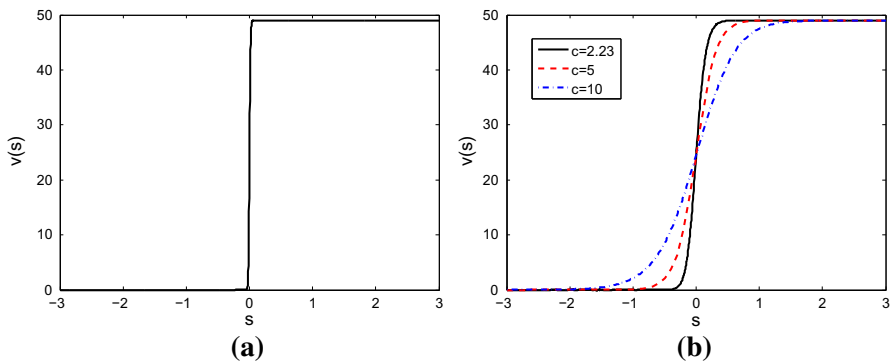**Fig. 7** Wave profiles when $a = 0$ and $c = 0.23$: **a** profile of $u(s)$; **b** profile of $w(s)$

Fig. 8 Wave profiles of $v(s)$ when $a = 0$: **a** $c = 0.23$; **b** $c = 0.23, 5, 10$

Fig. 9, we see that $w(s)$ and $v(s)$ go to negative for some values of s when $c = 5 > c^*$. This means for $c = 5$, there is no traveling wavefront for (14). In fact, numerical simulations show that this is also the case for $c \geq 13$. However, for $c = 14$, the system (14) has traveling wavefront (see Fig. 10). This implies that if the minimal wave speed exists, it is between 13 and 14. Obviously, this minimal wave speed is also different from the spreading speed $c = 1.547$ established in the preceding section. From these numerical results, we see that in the presence of repulsion effect, the linearized system will not determine the minimal wave speed for the original system, that it, the minimal wave speed is not linearly deterministic.

5 Conclusions and Discussion

In this paper, we propose a general virus infection dynamic model to describe the new mechanism reported in (Doceul et al. 2010) that can speed up the spread of virus within host. This new mechanism is called the repulsion of superinfecting virions by infected cells. Although this mechanism was discovered for vaccinia virus, it was pointed out in (Doceul et al. 2010) that some other viruses may also have this kind of
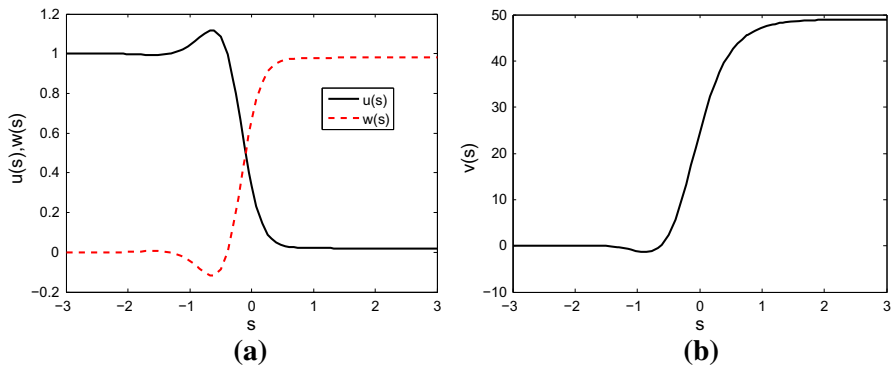
Fig. 9 For $a = 0.45$, when $c = 5$, there is no traveling wave solution, since $w(s)$ and $v(s)$ go to negative for some s
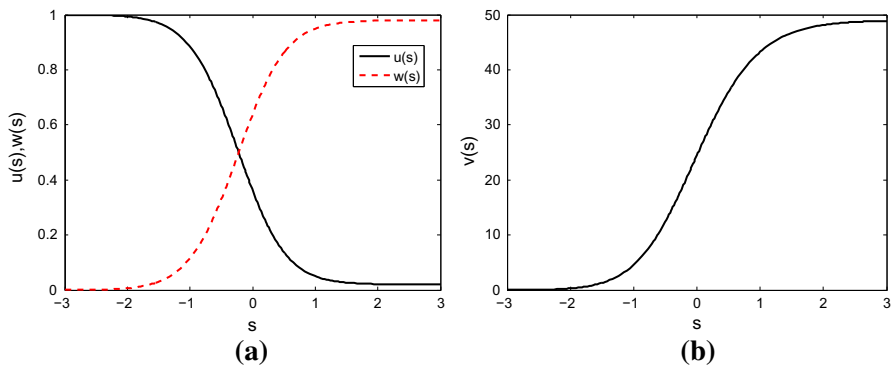

Fig. 10 For $a = 0.45$, when $c = 14$, there exists a traveling wave solution. **a** The wave profile of $u(s)$ and $w(s)$, **b** the wave profile of $v(s)$

rapid spreading mechanisms. With our general model, we have numerically confirmed the experimental results reported in Doceul et al. (2010), that is, the repulsion of superinfecting virions ($a > 0$) accelerates the spread of free viral particles. This model has the potential to be used for predicting the spreading speed for other viruses with similar repulsion effect.

In Sects. 3 and 4, we chose a specific diffusion function (11) for virus population. We can obtain similar results about spreading speed and traveling wave solutions for the following diffusion function:

$$D_V(I) = D_0 + kI, \qquad (26)$$

where $k > 0$. For example, choosing the same values for parameters and initial functions as that in Fig. 4, we see that the repulsion effect of infected cells on superinfecting virions also promotes the spread of viruses, as shown in Fig. 11. When there is no repulsion effect, the spreading speed is approximately $c = 0.2778$; while $c = 1.2222$, when the repulsion effect exists. On the other hand, note that the wave speed c^* does
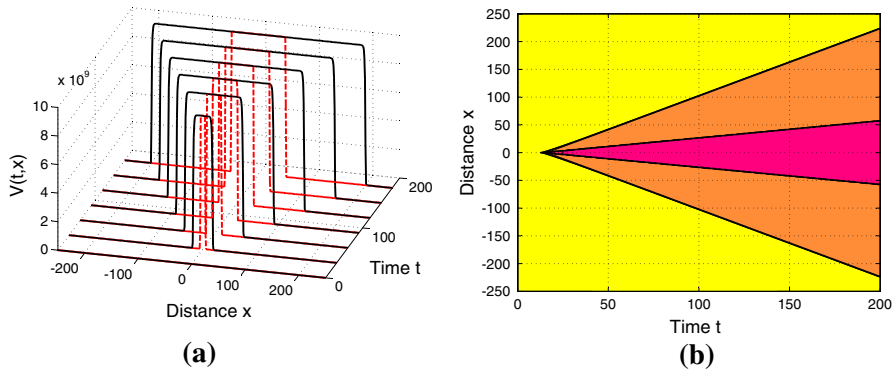
(a)   **(b)**

Fig. 11 **a** The evolution of $V(t, x)$ from the initial distribution $V_0(x)$, where *dashed line* (*red*): $k = 0$; *solid line* (*black*): $k = 0.38 \times 10^{-7}$. **b** The contour of (**a**) (Color figure online)

(a)   **(b)**
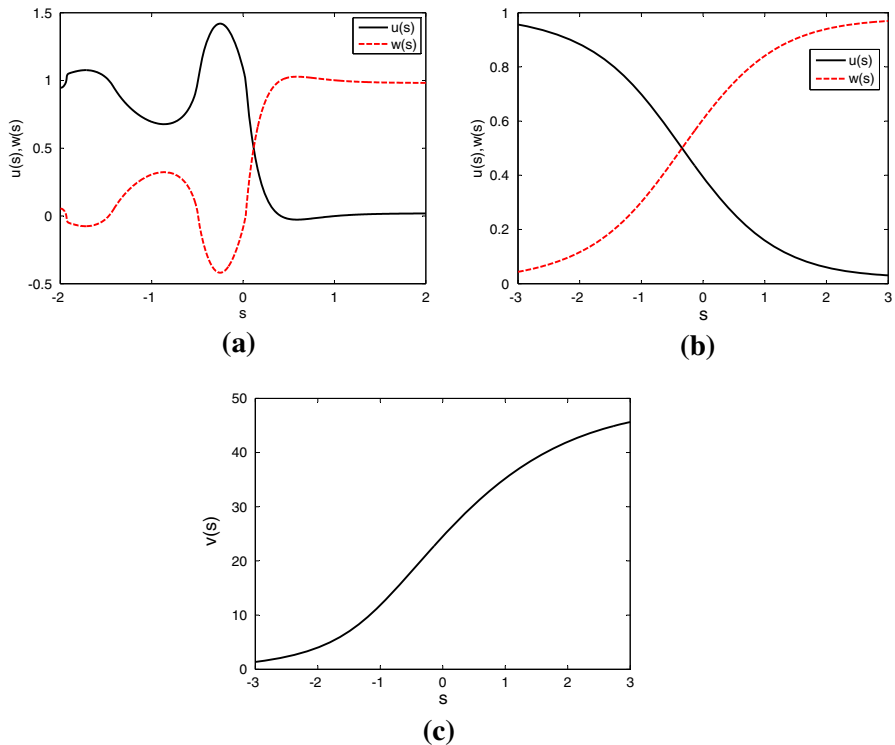

(c)

Fig. 12 For $k = 0.38 \times 10^{-7}$, **a** when $c = 10$, there is no traveling wave solution, since $w(s)$ goes to negative for some s; **b**, **c** when $c = 26$, there exists traveling wave solution

not depend on function $g(I)$. Hence, the existence of traveling wave solutions for $0 < c < c^*$ is same as the case of the diffusion function (11). When the repulsion effect exists and the diffusion function takes the form (26), we can also show numerically that the speed c^* is not the minimal wave speed (see Fig. 12) and the minimal

wave speed is also not consistent with the asymptotic spreading speed. For example, with the same parameters as that in Fig. 11, system (14) does not have traveling wave solution with speed $c = 10$ (see Fig. 12a), and this is true for $c \leq 25$. For $c = 26$, system (14) has traveling wave solutions (see Fig. 12b, c). Therefore, the minimal wave speed may be between 25 and 26 for rescaled system (14), and it may be between 2.5 and 2.6 for original system (13). This minimal wave speed is inconsistent with the spreading speed $c = 1.2222$.

In many mathematical and epidemiological models, especially for scalar equation or cooperative systems, the asymptotic spreading speed can be characterized as the slowest speed of traveling wave front solutions connecting an unstable steady state and a stable steady state (see, e.g., Li et al. 2005 and the references therein). Fisher's equation is such a model (classic). Such a result is very useful, since the slowest wave speed is easier to be calculated than the spreading speed.

As far as spreading speed goes, under some conditions, the linear determinacy holds for cooperative systems (Weinberger et al. 2002), that is, the spreading rate of the full nonlinear model agrees with the spreading rate of the system linearized about the leading edge of the invasion. For example, Lewis et al. (2002) obtained some parameter ranges for the Lotka–Volterra competition model, for which the spreading speed is linearly determined. They also derived a set of sufficient conditions for linear determinacy in a spatially explicit two-species discrete-time competition model. However, linear determinacy is not always valid, especially for complicated models, such as, competition models and prey–predator models. When linear determinacy does not hold, spread rates may exceed linearly determined predictions. There are also cases that different species in a model system may have different spreading speeds (Li et al. 2005; Weinberger et al. 2007). In our model, the linear determinacy does not hold and the spreading rate is much larger than linearly determined minimal wave speed in the presence of repulsion effect. This may be due to the complexity of the virus dynamic system, which is neither a cooperative system nor a competitive system. In fact, the target cell population and free virus population have a relationship similar to a prey–predator system, while infected cells and free viruses are cooperative. In our model, the minimal wave speed, given by the linearized analysis at infection-free steady state, is only true for the case when there is no repulsion effect ($a = 0$). If repulsion of superinfecting virions is present, the minimal wave speed would be much higher than the linearly determined wave speed.

Besides the classical route of cell-free virus spread, many viruses can spread through cell-to-cell transmission (Sattentau 2008), that is, viruses move between cells without diffusing through the extracellular environment. For instance, HIV-1 and HTLV-1 can spread from cell to cell by virological synapses or cell membrane nanotubes (Sattentau 2011); murine leukemia virus (MLV) can establish filopodial bridges for efficient cell-to-cell transmission (Mothes et al. 2010); Herpes simplex virus type-1 (HSV-1) can move between fibroblasts by polarized assembly and budding at basolateral intercellular junctions (Sattentau 2011); vaccinia virus can also spread through cell to cell by projection on actin tails (Sattentau 2008). We do not consider this route of spread in this paper and leave it for a separate research project.

Appendix 1

Proofs of Theorems 2.1 and 2.3

Proof of Theorem 2.1 Note that the system (5) is normally elliptic and triangular (in fact diagonal). According to Theorem 1 Amann (1989) or Theorems 14.4 and 14.6 in Amann (1993), (5)–(4) has a unique classical solution (T, I, V) defined on $[0, \tau_0) \times \Omega$ such that

$$(T, I, V) \in \mathbf{C}([0, \tau_0), \mathbf{X}_+) \cap \mathbf{C}^{2,1}((0, \tau_0) \times \bar{\Omega}, \mathbb{R}^3),$$

where $\tau_0 > 0$ is the maximal value for interval of existence of the solution. The nonnegativity of the solution follows from Theorem 15.1 by Amann (1993). In order to show that $\tau_0 = \infty$, by Theorem 5.2 in Amann (1989) and the nonnegativeness of the solution confirmed above, it suffices to prove that the solution (T, I, V) is bounded above by some positive values.

From the T and I equations in (2), we see that

$$\frac{\partial}{\partial t}(T + I) = D_T \Delta(T + I) + h(x) - d_T T - d_I I$$
$$\leq D_T \Delta(T + I) + \bar{h} - d_m(T + I),$$

where $\bar{h} = \max_{x \in \Omega} h(x)$ and $d_m = \min\{d_T, d_I\}$. By Lemma 1 in Lou and Zhao (2011), $\bar{h}/d_m$ is the globally attractive steady state for the scalar parabolic equations

$$\frac{\partial w(t, x)}{\partial t} = D_T \Delta w(t, x) + \bar{h} - d_m w(t, x), \quad x \in \Omega, \ t > 0,$$
$$\frac{\partial w(t, x)}{\partial v} = 0, \quad x \in \partial\Omega, \ t > 0.$$

The parabolic comparison theorem (Smith 1995, Theorem 7.3.4) implies that $T + I$ is bounded. This together with the nonnegativity of T and I further implies that both $T(t, x)$ and $I(t, x)$ are bounded. We assume $0 \leq T(t, x) \leq T_M, 0 \leq I(t, x) \leq I_M$.

Let $\bar{\gamma} = \max_{x \in \Omega}\{\gamma(x)\}$, and $V_M = \bar{\gamma} I_M / d_V$. For any given I, define the operator $\mathcal{P}$ by

$$\mathcal{P}V = V_t - \nabla \cdot (D_V(I)\nabla V) - \gamma(x)I + d_V V.$$

For any solution (T, I, V) of the system (2)–(3)–(4), we have $\mathcal{P}V = 0$. On the other hand,

$$\mathcal{P}V_M = d_V V_M - \gamma(x)I \geq d_V V_M - \bar{\gamma} I_M = 0 = PV.$$

On the boundary $\partial\Omega$, we have $\frac{\partial V_M}{\partial v} = 0$. Thus, $V = V_M$ is an upper solution of the V equation in the system (2)–(3). By the comparison principle, we obtain that $V(t, x) \leq V_M$. Therefore, the solution (T, I, V) is bounded, and hence, it exists globally.

Proof of Theorem 2.3 Linearizing (2) at $\bar{E} = (\bar{T}, \bar{I}, \bar{V})$ gives

$$\frac{\partial}{\partial t} u(t, x) = (\bar{D}\Delta + \bar{A})u(t, x),$$

where

$$\bar{D} = \begin{pmatrix} D_T & 0 & 0 \\ 0 & D_T & 0 \\ 0 & 0 & D_V(\bar{I}) \end{pmatrix}, \quad \bar{A} = \begin{pmatrix} -d_T - \beta\bar{V} & 0 & -\beta\bar{T} \\ \beta\bar{V} & -d_I & \beta\bar{T} \\ 0 & \gamma & -d_V \end{pmatrix}, \quad u = \begin{pmatrix} u_1 \\ u_2 \\ u_3 \end{pmatrix}.$$

The corresponding characteristic polynomial of this linearized system is

$$| \lambda I + \bar{D}k^2 - \bar{A} | = 0, \tag{27}$$

where k is the wavenumber, λ is the eigenvalue which determines temporal growth (Murray 2000). The positive steady state $\bar{E}$ is linearly stable if all eigenvalues have negative real parts.

Substituting the two matrices $\bar{A}$ and $\bar{D}$ into (27), we obtain

$$\begin{vmatrix} \lambda + D_T k^2 + d_T + \beta\bar{V} & 0 & \beta\bar{T} \\ -\beta\bar{V} & \lambda + D_T k^2 + d_I & -\beta\bar{T} \\ 0 & -\gamma & \lambda + D_V(\bar{I})k^2 + d_V \end{vmatrix} = 0,$$

that is,

$$\lambda^3 + b_1(k^2)\lambda^2 + b_2(k^2)\lambda + b_3(k^2) = 0, \tag{28}$$

where

$$\begin{aligned}
b_1(k^2) &= (2D_T + D_V(\bar{I}))k^2 + (d_T + d_I + d_V) > 0, \\
b_2(k^2) &= [D_T^2 + 2D_T D_V(\bar{I})]k^4 \\
&\quad + [D_T d_I + D_T(d_T + \beta\bar{V}) + D_T d_V + D_V(\bar{I})(d_T + \beta\bar{V}) + D_T d_V \\
&\quad + D_V(\bar{I})d_I]k^2 + (d_T + \beta\bar{V})d_I + (d_T + \beta\bar{V})d_V > 0, \\
b_3(k^2) &= D_T^2 D_V(\bar{I})k^6 + [D_T^2 d_V + D_T D_V(\bar{I})d_I + D_T D_V(\bar{I})(d_T + \beta\bar{V})]k^4 \\
&\quad + [D_T(d_T + \beta\bar{V})d_V + D_V(\bar{I})(d_T + \beta\bar{V})d_I]k^2 \\
&\quad + \beta\bar{V}d_I d_V > 0.
\end{aligned}$$

$$\begin{aligned}
&b_1(k^2)b_2(k^2) - b_3(k^2) \\
&= (2D_T + D_V(\bar{I}))[D_T^2 + 2D_T D_V(\bar{I})]k^6
\end{aligned}$$

$$+ \{[(2D_T + D_V(\bar{I}))][D_T d_I + (D_T + D_V(\bar{I}))(d_T + \beta\bar{V})$$
$$+ 2D_T d_V + D_V(\bar{I})d_I]$$
$$+ [D_T^2 + 2D_T D_V(\bar{I})](d_T + d_I + d_V)\}k^4$$
$$+ \{(2D_T + D_V(\bar{I}))[(d_T + \beta\bar{V})d_I + (d_T + \beta\bar{V})d_V]$$
$$+ [D_T d_I + (D_T + D_V(\bar{I}))(d_T + \beta\bar{V}) + 2D_T d_V$$
$$+ D_V(\bar{I})d_I](d_T + d_I + d_V)\}k^2$$
$$+ (d_T + d_I + d_V)[(d_T + \beta\bar{V})d_I + (d_T + \beta\bar{V})d_V]$$
$$- D_T^2 D_V(\bar{I})k^6 - [D_T^2 d_V + D_T D_V(\bar{I})d_I + D_T D_V(\bar{I})(d_T + \beta\bar{V})]k^4$$
$$- [D_T(d_T + \beta\bar{V})d_V + D_V(\bar{I})(d_T + \beta\bar{V})d_I]k^2$$
$$- \beta\bar{V}d_I d_V$$

$$\geq 4D_T^2 D_V(\bar{T})k^6 + \{2D_T[D_T d_I$$
$$+ D_V(\bar{I})(d_T + \beta\bar{V}) + 2D_T d_V + D_V(\bar{I})d_I] + [D_T^2 + 2D_T D_V(\bar{I})]d_T\}k^4$$
$$+ \{D_T[(d_T + \beta\bar{V})d_I + (d_T + \beta\bar{V})d_V]$$
$$+ [D_T d_I + (D_T + D_V(\bar{I}))(d_T + \beta\bar{V}) + 2D_T d_V + D_V(\bar{I})d_I](d_T + d_I + d_V)\}k^2$$
$$+ (d_T + d_I)[(d_T + \beta\bar{V})d_I + (d_T + \beta\bar{V})d_V]$$
$$> 0.$$

By the Routh–Hurwitz Criterion, we know that all eigenvalues of (28) have negative real parts, and therefore, the positive steady state $\bar{E}$ is linearly stable if it exists.

Appendix 2

Proof of nonexistence of traveling wavefront solutions for $c \in (0, c^*)$.

The Jacobian matrix of (16) at E_0' is

$$J_0 = \begin{pmatrix} -1/c & 0 & -1/c & 0 \\ 0 & -\rho_1/c & 1/c & 0 \\ 0 & 0 & 0 & 1 \\ 0 & -\rho_2/D_0 & \rho_3/D_0 & c/D_0 \end{pmatrix}.$$

It has an eigenvalue $\lambda = -1/c$ which is negative for all $c > 0$. So, we only need to consider other eigenvalues which are determined by

$$P(\lambda) := \lambda^3 + a_1\lambda^2 + a_2\lambda + a_3 = 0,$$

where

$$a_1 = \frac{D_0\rho_1 - c^2}{cD_0}, \quad a_2 = -\frac{\rho_1 + \rho_3}{D_0} < 0, \quad a_3 = \frac{\rho_2 - \rho_1\rho_3}{cD_0} > 0.$$

Since $P(0) = a_3 > 0$ and $P(-\infty) = -\infty$, $P(\lambda) = 0$ has a negative root. By the Descarte's rule of signs and by the Routh–Hurwitz criterion, the other two roots of $P(\lambda) = 0$ are either positive and real or a pair of conjugate complex numbers. In the latter case, the complex eigenvalues imply the oscillations of solutions of (16) near E_0', implying the w and v will take negative values (making solutions biologically meaningless), and thus, (16)–(17) cannot have positive solutions, meaning that (14) cannot have traveling wavefronts connecting E_0 and $\bar{E}$. Therefore, in order for (14) to have traveling wavefronts connecting E_0 and $\bar{E}$, it is necessary $P(\lambda) = 0$ to have a pair of positive real roots (counting multiplicity).

Note that $P'(\lambda) = 3\left(\lambda^2 + \frac{2a_1}{3}\lambda + \frac{a_2}{3}\right)$ and $P'(\lambda) = 0$ has a unique positive root

$$\lambda^* = \frac{1}{3}\left(-a_1 + \sqrt{a_1^2 - 3a_2}\right).$$

Since $P(0) = a_3 > 0$ and $P'(0) = a_2 < 0$, we conclude that $P(\lambda) = 0$ has two positive real roots if and only if $P(\lambda^*) < 0$. From $P'(\lambda^*) = 0$, we obtain that

$$\lambda^{*2} + \frac{2a_1}{3}\lambda^* + \frac{a_2}{3} = 0, \quad \lambda^{*3} + \frac{2a_1}{3}\lambda^{*2} + \frac{a_2}{3}\lambda^* = 0.$$

Using these equations to simplify the form of $P(\lambda^*)$, we obtain

$$\begin{aligned}
P(\lambda^*) &= \frac{a_1}{3}\lambda^{*2} + \frac{2a_2}{3}\lambda^* + a_3 \\
&= \frac{2}{3}\left(a_2 - \frac{a_1^2}{3}\right)\lambda^* + a_3 - \frac{a_1 a_2}{9} \\
&= \frac{1}{27}\left[-2\left(a_1^2 - 3a_2\right)^{3/2} + 27a_3 + 2a_1^3 - 9a_1 a_2\right].
\end{aligned}$$

It then follows that

$$\begin{aligned}
P(\lambda^*) < 0 &\Leftrightarrow 27a_3 + 2a_1^3 - 9a_1 a_2 \le 0, \text{ OR } 27a_3 + 2a_1^3 - 9a_1 a_2 \\
&> 0 \text{ AND } 4\left(a_1^2 - 3a_2\right)^3 > \left(27a_3 + 2a_1^3 - 9a_1 a_2\right)^2; \\
P(\lambda^*) > 0 &\Leftrightarrow 27a_3 + 2a_1^3 - 9a_1 a_2 > 0 \text{ AND } 4\left(a_1^2 - 3a_2\right)^3 \\
&< \left(27a_3 + 2a_1^3 - 9a_1 a_2\right)^2.
\end{aligned}$$

Let $Q_1(c) := 27a_3 + 2a_1^3 - 9a_1 a_2$, then $Q_1(c) = \frac{1}{D_0^3 c^3}(d_0 c^6 + d_1 c^4 + d_2 c^2 + d_3)$, where $d_0 = -2$, $d_1 = -3D_0(\rho_1 - 3\rho_3)$, $d_2 = 3D_0^2(9\rho_2 - 6\rho_1\rho_3 + \rho_1^2) > 0$ and $d_3 = 2\rho_1^3 D_0^3 > 0$. By the Descarte's rule of signs, $\bar{Q}_1(c) := d_0 c^6 + d_1 c^4 + d_2 c^2 + d_3 = 0$ has a unique positive root $c_0^* > 0$. Since $\bar{Q}_1(0) = d_3 > 0$, we see that $\bar{Q}_1(c) > 0$

if $0 < c < c_0^*$, and $\bar{Q}_1(c) < 0$ if $c > c_0^*$. Furthermore, $Q_1(c_0^*) = 0$, $Q_1(c) > 0$ if $0 < c < c_0^*$, and $Q_1(c) < 0$ if $c > c_0^*$.

Let $Q_2(c) := 4\left(a_1^2 - 3a_2\right)^3 - \left(27a_3 + 2a_1^3 - 9a_1a_2\right)^2$, then $Q_2(c) = \frac{27}{D_0^4 c^4}(b_0 c^6 + b_1 c^4 + b_2 c^2 + b_3)$ where b_i, $i = 0, 1, 2, 3$, are given by (18).

Note that $b_0 > 0$, $b_1 > 0$, $b_3 < 0$. Again by the Descarte's rule of signs, $Q(c)$ given by (18) has a unique positive root $c^* > 0$. Since $Q(0) = b_3 < 0$, we see that $Q(c) < 0$ if $0 < c < c^*$, and $Q(c) > 0$ if $c > c^*$. Therefore, $Q_2(c^*) = 0$, $Q_2(c) < 0$ if $0 < c < c^*$, and $Q_2(c) > 0$ if $c > c^*$.

Note that $a_1^2(c) - 3a_2 > 0$ for all $c > 0$. Thus, $Q_2(c_0^*) = a_1^2(c_0^*) - 3a_2 > 0$, implying $c^* < c_0^*$. In summary, we have obtained:

$$\begin{aligned}
P(\lambda^*) < 0 &\Leftrightarrow Q_2(c) \le 0, \ \ \text{OR}, \ \ Q_2(c) > 0 \ \text{AND} \ Q_1(c) > 0 \\
&\Leftrightarrow c \ge c_0^* \ (\text{hence } c > c^*), \ \ \text{OR}, \ \ 0 < c < c_0^* \ \text{AND} \ c > c^* \\
&\Leftrightarrow c > c^*; \\
P(\lambda^*) > 0 &\Leftrightarrow Q_2(c) > 0 \ \text{AND} \ Q_1(c) < 0 \\
&\Leftrightarrow 0 < c < c_0^* \ \text{AND} \ c < c^* \\
&\Leftrightarrow 0 < c < c^*.
\end{aligned}$$

Thus, for any $c \in (0, c^*)$, system (14) has no traveling wavefront solutions with speed c that connects E_0 and $\bar{E}$.

From the definition of $Q(c)$, we obtain

$$Q(\sqrt{D_0\rho_1}) = D_0^3 \rho_1 \left[4\rho_1(\rho_1 + \rho_3)^3 - 27(\rho_2 - \rho_1\rho_3)^2\right].$$

It is easy to see that $Q_3(\rho_1) := 4\rho_1(\rho_1 + \rho_3)^3$ is strictly increasing function of ρ_1, and $Q_3(0) = 0$, $Q_3(+\infty) = +\infty$; $Q_4(\rho_1) := 27(\rho_2 - \rho_1\rho_3)^2$ is strictly decreasing function of ρ_1 when $\rho_2 > \rho_1\rho_3$, and $Q_4(0) = 27\rho_2^2$. Therefore, $Q(\sqrt{D_0\rho_1})$ has a unique positive root ρ_1^*, such that $Q(\sqrt{D_0\rho_1}) < 0$ for $0 < \rho_1 < \rho_1^*$, and $Q(\sqrt{D_0\rho_1}) > 0$ for $\rho_1 > \rho_1^*$. By the property of $Q(c)$, we have $\sqrt{D_0\rho_1} < c^*$ for $0 < \rho_1 < \rho_1^*$; $\sqrt{D_0\rho_1} > c^*$ for $\rho_1 > \rho_1^*$ and $c^* = \sqrt{D_0\rho_1^*}$, where ρ_1 is determined by (21). Therefore, we obtain the information (20) about c^*.

References

Adams RA (1975) Sobolev spaces. Academic Press, New York

Amann H (1989) Dynamical theory of quasilinear parabolic equations III: global existence. Math Z 202:219–250

Amann H (1993) Nonhomogeneous linear and quasilinear elliptic and parabolic boundary value problems. In: Schmeisser HJ, Triebel H (eds) Function spaces, differential operators and nonlinear analysis (Friedrichroda, 1992), vol 133. Teubner-Texte zur Mathematik. Teubner, Stuttgart, pp 9–126

Beyn WJ (1990) The numerical computation of connecting orbits in dynamical systems. IMA J Numer Anal 9:379–405

Bonhoeffer S, May RM, Shaw GM, Nowak MA (1997) Virus dynamics and drug therapy. Proc Natl Acad Sci USA 94:6971

Chatelin F (1981) The spectral approximation of linear operators with application to the computation of eigenelements of differential and integral operators. SIAM Rev 23:495–522

Condit RC (2010) Surf and turf: mechanism of enhanced virus spread during poxvirus infection. Viruses 2:1050–1054

Doceul V, Hollinshead M, van der Linden L, Smith GL (2010) Repulsion of superinfecting virions: a mechanism for rapid virus spread. Science 327:873–876

Gan Q, Xu R, Yang P (2010) Travelling waves of a hepatitis B virus infection model with spatial diffusion and time delay. J Appl Math 75:392–417

Guo Z, Wang F-B, Zou X (2012) Threshold dynamics of an infective disease model with a fixed latent period and non-local infections. J Math Biol 65:1387–1410

Haberman R (1998) Elementary applied partial differential equations: with Fourier series and boundary value problems. Prentice Hall, New Jersey

Heffernan JM, Smith RJ, Wahl LM (2005) Perspectives on the basic reproductive ratio. J R Soc Interface 2(4):281–293

Ikebe Y (1972) The Galerkin method for the numerical solution of Fredholm integral equations of the 2nd kind. SIAM Rev 14:465–491

Komarova NL (2007) Viral reproductive strategies: how can lytic viruses be evolutionarily competitive? J Theor Biol 249:766–784

Korobeinikov A (2004) Global properties of basic virus dynamics models. Bull Math Biol 66:879–883

Li B, Weinberger HF, Lewis MA (2005) Spreading speeds as slowest wave speeds for cooperative systems. Math Biosci 196:82–98

Lewis MA, Li B, Weinberger HF (2002) Spreading speeds and linear determinacy for two-species competition models. J Math Biol 45:219–233

Lou Y, Zhao XQ (2011) A reaction–diffusion malaria model with incubation period in the vector population. J Math Biol 62:543–568

Mothes W, Sherer NM, Jin J, Zhong P (2010) Virus cell-to-cell transmission. J Virol 84:8360–8368

Murray JD (2000) Mathematical biology II: spatial models and biomedical applications. Springer, New York

Neubert MG, Parker IM (2004) Projecting rates of spread for invasive species. Risk Anal 24:817–831

Sattentau Q (2008) Avoiding the void: cell-to-cell spread of human viruses. Nat Rev Microbiol 6:815–826

Sattentau Q (2011) The direct passage of animal viruses between cells. Curr Opin Virol 1:396–402

Smith HL (1995) Monotone dynamic systems: an introduction to the theory of competitive and cooperative systems. Math Surveys Monogr, vol 41. American Mathematical Society, Providence, RI

Thieme HR (2009) Spectral bound and reproduction number for infinite-dimensional population structure and time heterogeneity. SIAM J Appl Math 70:188–211

Vaidya NK, Wang F-B, Zou X (2012) Avian influenza dynamics in wild birds with bird mobility and spatial heterogeneous environment. Discrete Cont Dyn Syst B 17:2829–2848

Wang K, Wang W (2007) Propagation of HBV with spatial dependence. Math Biosci 210:78–95

Wang W, Zhao XQ (2011) A nonlocal and time-delayed reaction–diffusion model of dengue transmission. SIAM J Appl Math 71:147–168

Wang W, Zhao XQ (2012) Basic reproduction numbers for reaction diffusion epidemic models. SIAM J Appl Dyn Sys 11:1652–1673

Weinberger HF, Lewis MA, Li B (2002) Analysis of linear determinacy for spread in cooperative models. J Math Biol 45:183–218

Weinberger HF, Lewis MA, Li B (2007) Anomalous spreading speeds of cooperative recursion systems. J Math Biol 55:207–222

Xu R, Ma Z (2009) An HBV model with diffusion and time delay. J Theor Biol 257:499–509